Lithuanian Journal of Physics
Vol. **66**, No. 2, pp. 82–90 (2026)
ISSN 1648-8504 eISSN 2424-3647
DOI: https://doi.org/10.3952/physics.2026.66.2.3

COMPLEX OF $TPPS_4$ AND *L*-ASCORBIC ACID: PROTONATION OF THE PORPHYRIN CENTRE

A. Maršalka [a], A. Gruodis [a], and S. Bagdonas [b]

[a] *Institute of Chemical Physics, Faculty of Physics, Vilnius University, Saulėtekio 9, 10222 Vilnius, Lithuania*
[b] *Laser Research Center, Faculty of Physics, Vilnius University, Saulėtekio 9, 10222 Vilnius, Lithuania*
Email: alytis.gruodis@ff.vu.lt

Received 1 December 2025; accepted 21 January 2026

The *L*-ascorbic acid and $TPPS_4$ complex in water is treated as a close contact associate (intermolecular distance <0.2 nm). The paper presents the modelling of the structures and electronic excitations of two types of complexes using quantum-chemical methods. In both complexes, *L*-ascorbic acid acts as a reducing agent. In the second complex [*L*-ascorbic acid + $TPPS_4$ + *L*-ascorbic acid], intermolecular charge transfer occurs. Protonation of the $TPPS_4$ centre can be realized by connecting two *L*-ascorbic acid molecules as proton sources. The presence of *L*-ascorbic acid in the solvent enables an efficient protonation of the primary structure: $TPPS_4 \rightarrow H_2TPPS_4$.

Keywords: *L*-ascorbic acid, $TPPS_4$, protonation, theoretical models

1. Introduction

Tetrakis (4-sulfonatophenyl) porphyrin ($TPPS_4$, H_2TSPP, see Fig. 1(a)) represents a heterocyclic compound consisting of naturally occurring porphyrins. Over the last four decades, $TPPS_4$ has been used for several purposes: (i) in cancer therapy for photodynamic therapy as a potential photosensitizer to produce singlet oxygen; (ii) in biosensing for detecting HOOH and glucose; (iii) for single-molecule electronics etc. *L*-ascorbic acid (vitamin C, hexuronic acid, see Fig. 1(b)) represents a well-known organic material of high biological importance. *L*-ascorbic acid could be used for two reasons: a) as an antioxidant to help protect against oxidative stress in tissues and inflammation [1], and b) as a reducing agent and antioxidant in the synthesis of nanomaterials [2].

The combined use of $TPPS_4$ and *L*-ascorbic acid in the same media has been part of research for the last decade. Firstly, *L*-ascorbic acid (acting as an antioxidant) can increase the stability of $TPPS_4$ in several chemical reactions [3]. Secondly, *L*-ascorbic acid (A) can act as a reducing agent [4]:

$$A + 2H^+ + 2e^- = H_2A. \quad (1)$$

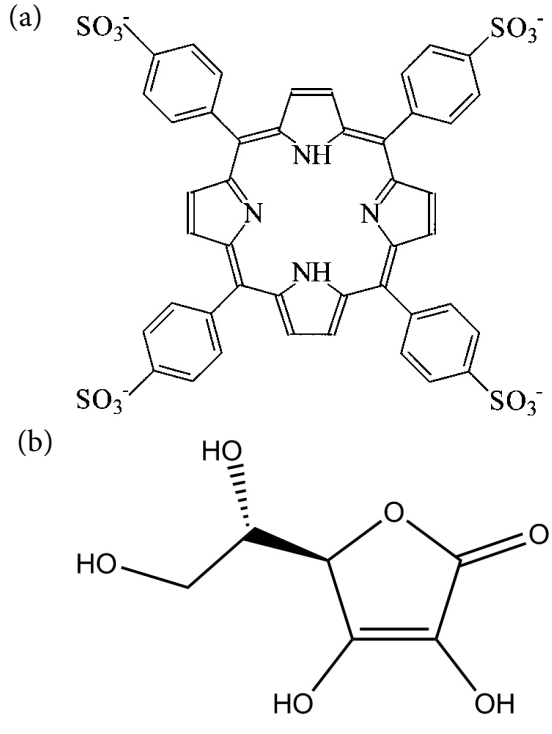

Fig. 1. (a) Tetrakis (4-sulfonatophenyl) porphyrin ($TPPS_4$, H_2TSPP). (b) *L*-ascorbic acid (vitamin C, hexuronic acid).

The exact mechanism of interaction between $TPPS_4$ and *L*-ascorbic acid is complex and only partially described. Specific conditions, such as

surrounding pH, pK, temperature, and the first and second solvation shells of the medium, must be considered.

This work is devoted to the simulation of possible structures of $TPPS_4$ and *L*-ascorbic acid (vitamin C) in water using quantum-chemical methods. The research hypothesis was formulated as follows: a) to estimate the stability conditions when the surrounding medium is close to neutral pH = 7; b) to estimate the role of electronic excitations for $TPPS_4$.

2. Literature review

2.1. $TPPS_4$ for photodynamic therapy

$TPPS_4$ is important in photodynamic therapy due to its effectiveness and versatility as a photosensitizer. Excellent solubility and biocompatibility allow the generation of reactive oxygen species (ROS) for tumour destruction *in vivo*. Lapes et al. [5] described a successful apoptosis of breast cancer using photodynamic therapy with a dose of <0.3 mg of $TPPS_4$, a light wavelength 630 nm, a fluence rate of <680 mW cm^{-2}, and a fluence of 150 J cm^{-2}. Advantages of the presented method include a high tumour concentration of $TPPS_4$ and a low total $TPPS_4$ dose. Jia et al. [6] reported a study evaluating the biological behaviour of $TPPS_4$ for tumour-targeted therapy. The authors claim that vitamin C could increase its stability *in vitro*. Generally, $TPPS_4$ is non-toxic in the dark. This means that normal tissues remain largely unharmed, providing an excellent therapeutic window.

$TPPS_4$ shows a preferential accumulation in tumour cells due to the potential for electrostatic targeting. Four sulfonate fragments can interact with positively charged biomolecules, often overexpressed on cancer cells. Binder et al. [7] analyzed a strong phototoxic effect leading to cell apoptosis at several radiation doses and six concentrations of the photosensitizers $TPPS_4$ and $MgTPPS_4$. They hypothesize that an irradiation dose of 1 J cm^{-2} is sufficient to provoke DNA fragmentation. Pessoto et al. [8] studied the influence of the porphyrin metal centre and meso ligands on the biological effects of meso-tetrakis porphyrins.

$TPPS_4$ could be used in the drug delivery systems [9] using conjugation to a nanoparticle. Creating hybrid systems with enhanced targeting properties allows for deeper tumour penetration. Conjugation of graphene oxide as a coating material for gold nanorods to $TPPS_4$ improves their phototherapeutic properties.

In molecular mechanistic studies, $TPPS_4$ is very useful due to its stable structure and sufficient fluorescence yield. Such behaviours allow us to study ROS-based mechanisms in cancer cell apoptosis using the interaction between porphyrins and biomolecules.

2.2. L-ascorbic acid as an antioxidant

Nowak et al. [10] investigated the properties of *L*-ascorbic acid in the presence of Fe^{2+}/Fe^{3+} ions and H_2O_2. It was concluded that *L*-ascorbic acid can act as a prooxidant. In that case, the formation of hydroxyl radicals (•OH) accelerates. Gamov et al. [11] analyse the reductive properties of ascorbate, which depend significantly on the dissociation of *L*-ascorbic acid, which, in turn, is influenced by the ionic strength value.

Marsalka et al. [12] analysed the model system to monitor the effects of *L*-ascorbic acid on oxygen-dependent photoreactions in aqueous solutions at different pH. It was shown that *L*-ascorbic acid suppresses (auto)photooxidative reactions but facilitates the photoinduced formation of phlorin-type photoproducts, thereby exhibiting a dual antioxidative and reducing activity in the presence of a hematoporphyrin-type photosensitizer.

2.3. Previous quantum chemical simulations

Simulations of chemical structures can be performed within the required framework (gas or solution phase) using density functional theory (DFT) methods. Bichara et al. [13] studied *L*-ascorbic acid in the described manner. Three stable molecules for the compound have been theoretically determined in the gas phase, and only an average of 2 additional stable conformations are present in the solid phase, as experimentally observed. They presented a complete assignment of all the observed bands in the infrared spectrum for *L*-ascorbic acid. Magar et al. [14] analyzed *L*-ascorbic acid at the B3LYP/6-311G(d,p) level. Examining HOMO–LUMO energy provided insights into chemical stability with an energy gap of 5.65 eV. It was found that the compound with such a large HOMO–LUMO gap is comparatively rigid. Berg [15] calculated the local minima of *L*-ascorbic acid using a density-functional approach.

Dabbagh et al. [16] theoretically studied the structures, stabilities, conformational analysis, and electronic transitions of *L*-ascorbic acid anions (four stereoisomers). It was observed that the deprotonation at the C5 site of two stereoisomers leads to the ring opening in both phases. Isomerization of the *L*-form to one of the *D*-form was observed during the optimization of the anions at C5.

Ebrahimi et al. [17] reported a conformational analysis of vitamin C using the second-order Møller–Plesset perturbation theory (MP2) with the correlation-consistent aug-cc-pVDZ basis set. They claim that hydrogen bond formation was responsible for the stability of most local minima on the potential energy surface and for the formation of cooperative networks.

In our group, several models for a very effective cytotoxicity for tumour cells *in vitro* using the mixtures of vitamin C and vitamin K_3 were analyzed [18, 19]. Development of novel therapies for hepatocellular carcinoma (HCC) is very important. Treatment of mouse hepatoma MH-22A cells with vitamin C and vitamin K_3 at a 100:1 ratio greatly enhanced cytotoxicity. When vitamins C and K_3 were combined at the same concentrations, they killed more than 90% of tumour cells. The mechanism of intermolecular charge transfer was created as the basic mechanism for neighbours' interactions.

3. Original part

3.1. Structures and simulation methods

$TPPS_4$ (with formula $C_{44}H_{30}N_4$, IUPAC name 5,10,15,20-tetrakis(4-sulfonatophenyl)porphyrin and *L*-ascorbic acid (with formula $C_6H_8O_6$, IUPAC name (5*R*)-[(1*S*)-1,2-dihydroxyethyl]-3,4-dihydroxyfuran-2(5*H*)-one) were used for quantum chemical simulations. Table 1 lists the chemical structures used in the simulations.

Simulations of ground-state molecular structure and corresponding electronic excitations have been provided using the Gaussian16 [20] package. Optimization of the ground electronic state has been provided using the semiempirical CAM-B3LYP method and the 6-31G(d) basis set, consisting of the polarization function (d). Electronic excitations were calculated using the semiempirical TD method for singlets only. Environmental effects were included using the PCM(water) routine for structure simulations as well as for excitations. The polarizable continuum model (PCM) is a widely used method for modelling solvation effects.

3.2. Results and discussion

Figure 2(a, b) represents the parameters of the simulated structures of M1 and M2 when a different behaviour of centre protonation is present. For M1, two native protons are located; for M2, four protons (two native plus two additional) are located. The M1 structure is practically flat, but the M2 structure is presented in a bend format. The bending angle (between the long axis of the pentaring and the central plane surface) is less than 30° degrees. Figure 3(a, b) represents the XY and XZ projections of simulated structures: M4 = M3 + M1 and M5 = M3 + M1 + M3, respectively. Short intermolecular contacts (less than 0.2 nm) occur between TPPS4 and *L*-ascorbic acid when the proton of *L*-ascorbic acid from position 4 or 5 could be shared between *L*-ascorbic acid and $TPPS_4$. In the case of M4 = M3 + M1 (see Fig. 3(a)), *L*-ascorbic acid loses one proton because the proton is in the near surroundings of the pentaring of $TPPS_4$. In the case of M5 = M3 + M1 + M1 (see Fig. 3(b)), both monomers of *L*-ascorbic acid (M1 from both sides) lose two protons (each one only). In that case, the reaction product contains an M2 structure (centre protonated, H_2TPPS_4) and two monomers of *L*-hydroascorbic acid.

Figure 4 represents the hybrid molecular orbitals (MOs) for complexes M4 (left) and M5. MOs such as nextLUMO, LUMO, HOMO, and nextHOMO play a very important role in all chemical reactions

Table 1. List of chemical structures.

N	Abbreviation	Charge	Chemical name and description	
1	M1	–4	Monomer, $TPPS_4$, centre-unprotonated	
2	M2	–2	Monomer, H_2TPPS_4, centre-protonated	
3	M3	0	Monomer, *L*-ascorbic acid	
4	M4	–4	Complex, M3+M1	*L*-ascorbic acid + $TPPS_4$
5	M5	–4	Complex, M3 + M1 + M3	*L*-ascorbic acid + $TPPS_4$ + *L*-ascorbic acid

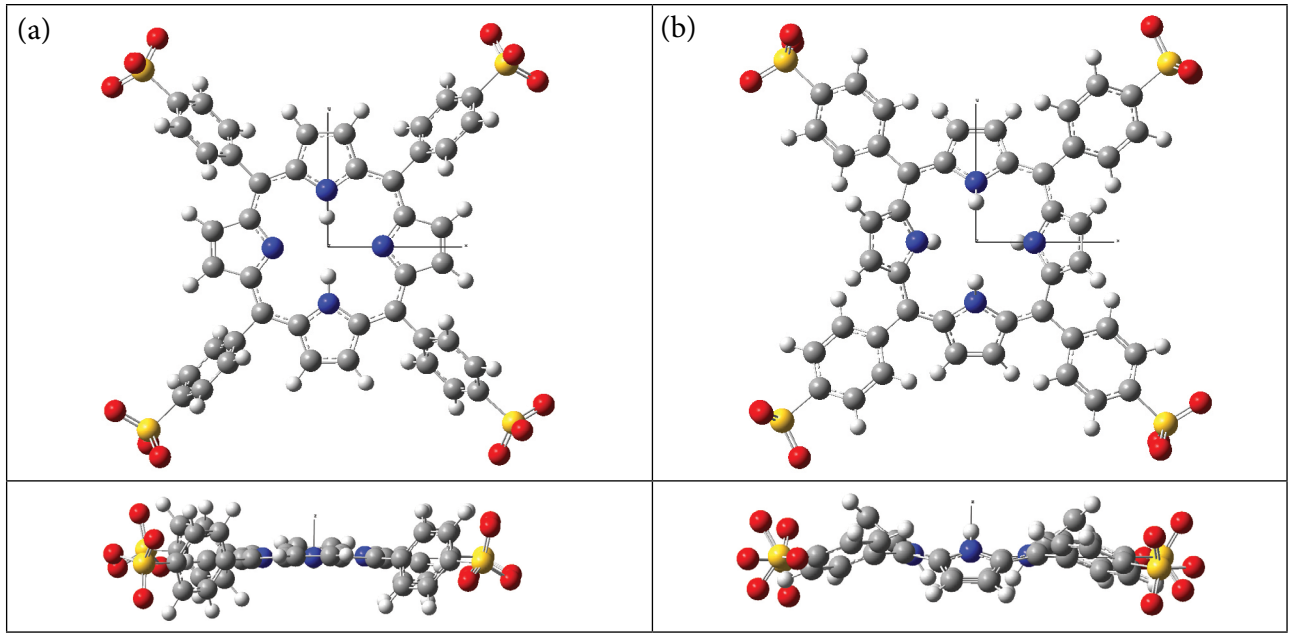

Fig. 2. (a) M1, centre unprotonated $TPPS_4$. XY (top) and XZ (bottom) projections. Structures after optimization using the CAM-B3LYP/6-31G(d) method. Solvation effects using PCM(water) were included. (b) M2, centre protonated H_2TPPS_4. XY (top) and XZ (bottom) projections. Structures after optimization using the CAM-B3LYP/6-31G(d) method. Solvation effects using PCM(water) were included.

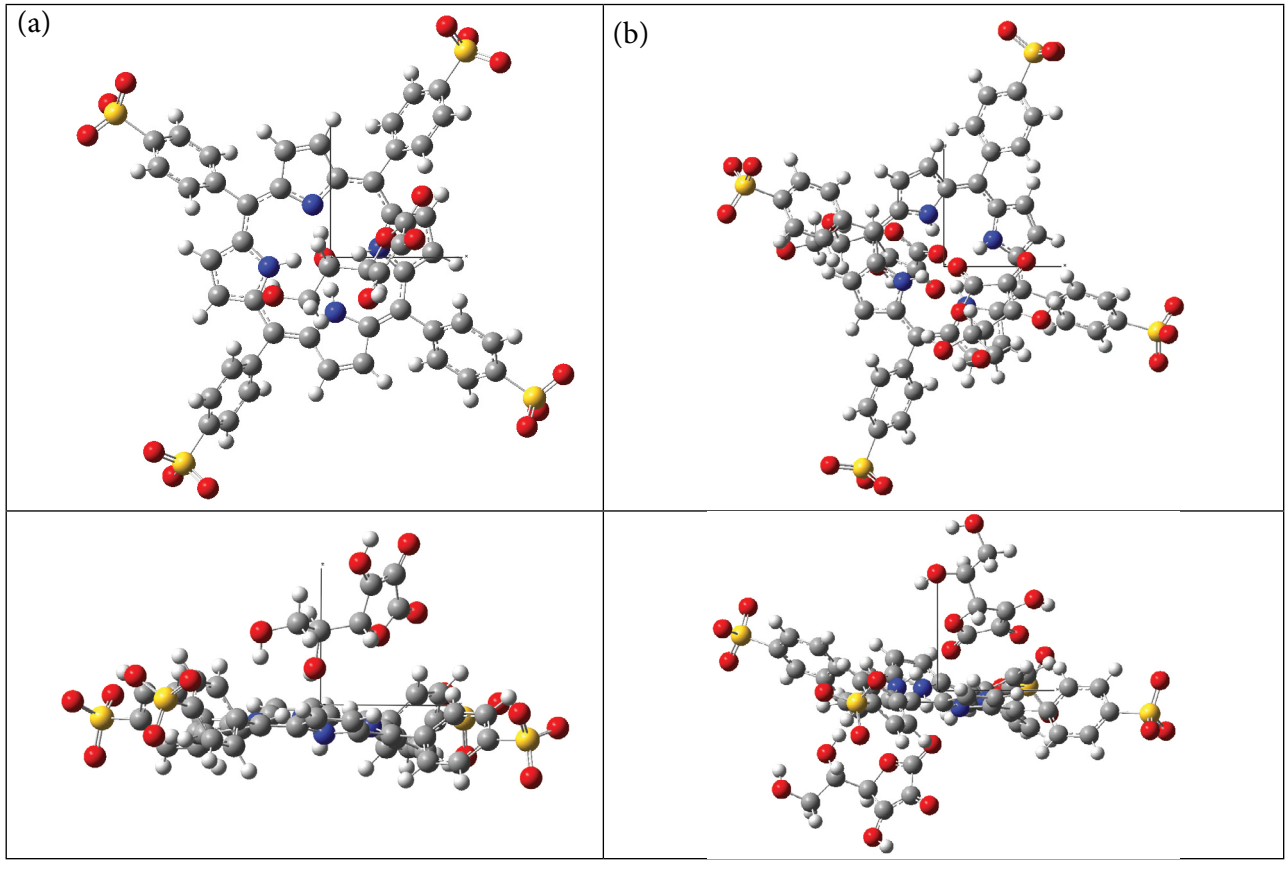

Fig. 3. (a). M4, complex, M3 + M1. XY (top) and XZ (bottom) projections. Structures after optimization using the CAM-B3LYP/6-31G(d) method. Solvation effects using PCM(water) were included. (b) M5, complex, M3 + M1 + M3. XY (top) and XZ (bottom) projections. Structures after optimization using the CAM-B3LYP/6-31G(d) method. Solvation effects using PCM(water) were included.

MOs	M4, complex, M3 + M1	MOs	M5, complex, M3 + M1 + M3
290	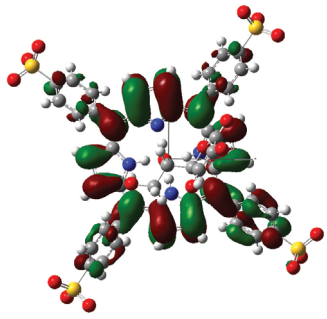	336	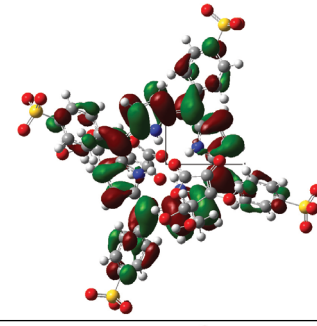
289, L	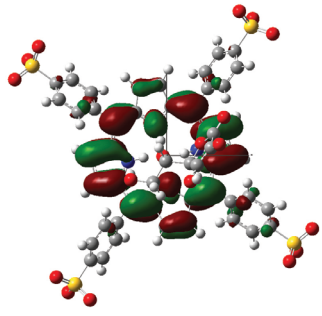	335, L	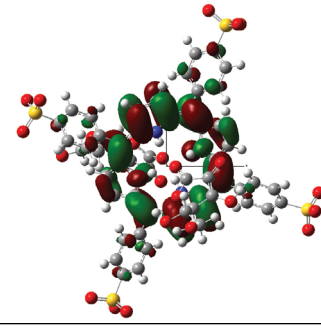
288, H	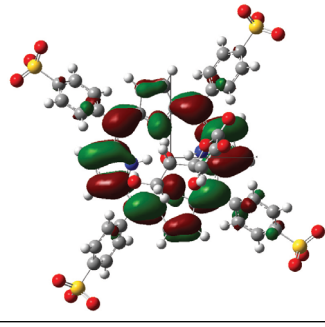	334, H	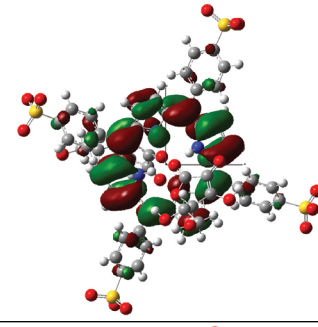
287	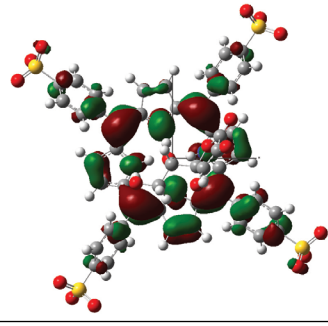	333, XY	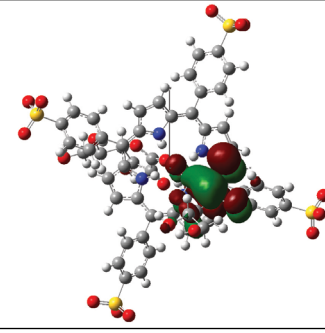
		333, XZ	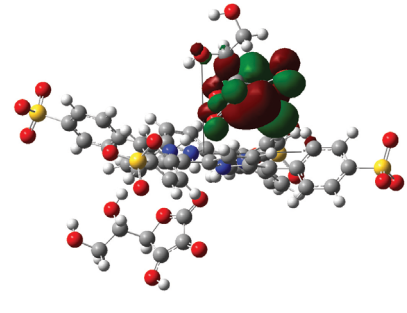

Fig. 4. Hybrid molecular orbitals MOs (nextLUMO, LUMO, HOMO, nextHOMO) for complexes M4 (left) and M5. For MO333, two projections – XY and XZ – are presented. Excitations were calculated using the semi-empirical TD method (for singlets). Structures after optimization using the CAM-B3LYP/6-31G(d) method. Solvation effects using PCM(water) were included.

and can be used to estimate molecular stability. Such MOs were calculated using a semiempirical TD method (for singlets). Structures optimized using the CAM-B3LYP/6-31G(d) method were used. Solvation effects using PCM(water) were included. For the M4 complex (*L*-ascorbic acid + $TPPS_4$), HOMO, LUMO, nextHOMO, and nextLUMO represent the charge distribution in $TPPS_4$. For the M5 complex (*L*-ascorbic acid + $TPPS_4$ + *L*-ascorbic acid), HOMO, LUMO, and nextLUMO represent charge distribution in $TPPS_4$, but nextHOMO represents charge distribution in *L*-ascorbic acid. In the case of two *L*-ascorbic acids, the M5 complex is involved in intermolecular charge transfer between two molecular units.

Table 2 represents the population of the lowest 'spectroscopic' states of complexes M4 and M5/*in aqua*. Two state parameters, such as transition energy Ene_x (eV) and oscillator strength Osc_x, were presented for the simulated electronic excitations. The semiempirical TD method (for singlets) was used. Environmental effects were included using the PCM(water) method. The structure M4 (*L*-ascorbic acid + $TPPS_4$) could be titled as an intermediate structure because one proton (lost from *L*-ascorbic acid, from position 5 or 6) cannot create a fully protonated centre. For M4, the allowed transition at 1.85 eV (oscillator strength 0.162) is quite the same as in the case of M1. It means that *L*-ascorbic acid is present only as a weak associate.

Two protons are necessary from *L*-ascorbic acid. Unfortunately, the partial fixation of *L*-hydroascorbic acid does not allow one to rotate the *L*-hydroascorbic acid to another position that is suitable for the removal of the second proton (from position 5 or 6). In that case, the second *L*-ascorbic acid is necessary, as presented in Fig. 3(b). The structure M5 (*L*-ascorbic acid + $TPPS_4$ + *L*-ascorbic acid) could be titled as the complex where intermolecular charge distribution occurs. For M5, Table 3 represents the expanded parameters of electronic excitations simulated using the semiempirical TD method (for singlets). *Simulation* represents the population of 'spectroscopic' states (from ground to excited) ΔE_n and a corresponding set of MOs with the contribution coefficient *k* (contribution of the respective excitation to the configurational interaction wavefunction). Figure 5 represents the population of 'spectroscopic' states (from ground to excited) for the most promising structure M5. For

Table 2. Simulated electronic excitations of complexes M4 and M5/*in aqua:* population of the lowest 'spectroscopic' states, transition energy Ene_x (eV) and oscillator strength Osc_x. Gaussian16, TD(nstate = 6, singlets) PCM(water) sp.

Name	Charge	Ene1 Osc1	Ene2 Osc2	Ene3 Osc3	Ene4 Osc4	Ene5 Osc5	Ene6 Osc6
M4	–4	0.65 0.001	1.45 0.018	**1.85** **0.162**	1.88 0.000	2.09 0.034	2.39 0.044
M5	–4	0.67 0.002	1.17 0.029	**1.35** **0.194**	1.62 0.006	1.89 0.024	1.96 0.023

Table 3. Parameters of electronic excitations simulated using the semiempirical TD method (for singlets). *Simulation* represents the population of 'spectroscopic' states (from ground to excited) ΔE_n and the corresponding set of MO with the contribution coefficient *k* (contribution of the respective excitation to the configurational interaction wavefunction).

M5	Transition	*Simulation*				
		ΔE, eV	λ, nm	Oscillator strength	Transition between MO	*k*
	$S_0 \rightarrow S_1$	0.67	1846	0.002	334 → 336	0.9802
	$S_0 \rightarrow S_2$	1.17	1058	0.029	331 → 335	0.7891
	$S_0 \rightarrow S_3$	1.35	919	0.194	331 → 334	0.8957
	$S_0 \rightarrow S_4$	1.62	767	0.006	332 → 334	09375
	$S_0 \rightarrow S_5$	1.89	653	0.024	300 → 333	0.5932
	$S_0 \rightarrow S_6$	1.96	632	0.023	330 → 334	0.7975

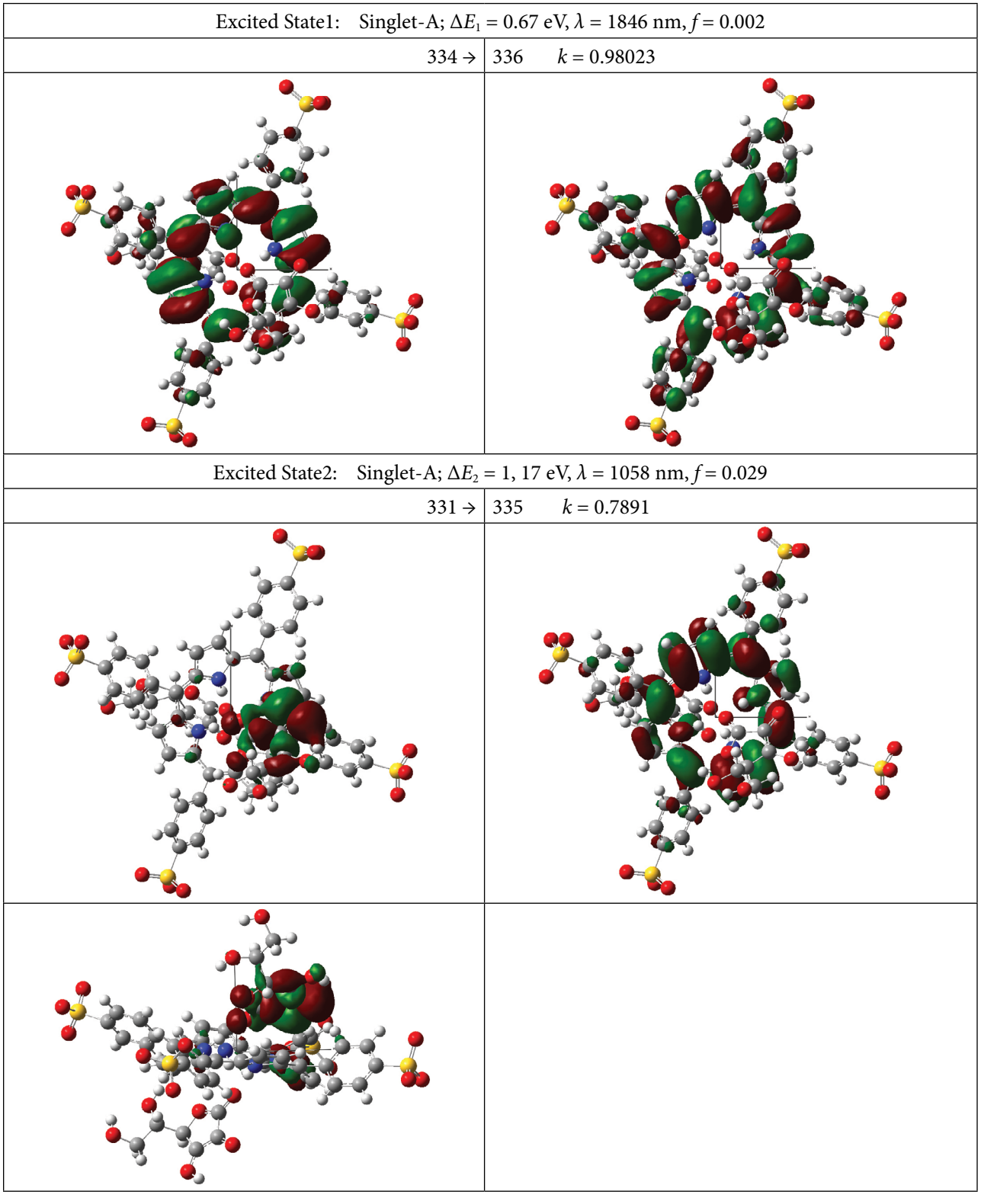

Fig. 5. M5. Population of the 'spectroscopic' states (from ground to excited).

the population, the first excited state $S_0 \rightarrow S_1$, corresponding to charge redistribution between MOs 334–336, occurs, which is typical of the centre-protonated structure M2, H_2TPPS_4, but not for the centre-unprotonated structure M1, $TPPS_4$. For the population, the second excited state $S_0 \rightarrow S_2$ corresponds to charge redistribution between MOs 331–335, which represents intermolecular charge transfer between *L*-hydroascorbic acid and $TPPS_4$.

4. Conclusions

Simulation of molecular structures using quantum-chemical methods allows us to estimate the most probable structures of the separate monomers, *L*-ascorbic acid and $TPPS_4$, as well as the complexes. The initial hypothesis that *L*-ascorbic acid acts as a reducing agent when in contact with $TPPS_4$ was confirmed. In the complex [*L*-ascorbic acid + $TPPS_4$ + *L*-ascorbic acid], intermolecular charge transfer takes place. Protonation of the centre of $TPPS_4$ could be provided using two *L*-ascorbic acids as the proton sources. The presence of *L*-ascorbic acid in the solvent allows a protonation reaction in the form of $TPPS_4 \rightarrow H_2TPPS_4$.

Acknowledgements

The authors are grateful to Prof. Ričardas Rotomskis for his essential advice and inspiration. Computations were performed on resources at the High-Performance Computing Center 'HPC Saulėtekis' (Faculty of Physics, Vilnius University, Lithuania).

References

[1] E.A. Abdulhameed, K.G.A. Rani, F.M. AlGhalban, E.A. Abou Neel, N. Khalifa, K.A. Khalil, M. Omar, and A.R. Samsudin, Managing oxidative stress using vitamin C to improve biocompatibility of polycaprolactone for bone regeneration *in vitro*, ACS Omega **9**(29), 31776–31788 (2024), https://doi.org/10.1021/acsomega.4c02858

[2] B.M.M. May, S. Parani, and O.S. Oluwafemi, Detection of ascorbic acid using green synthesized $AgInS_2$ quantum dots, Mater. Lett. **236**, 432–435 (2019), https://doi.org/10.1016/j.matlet.2018.10.155

[3] C. Li, X. Ding, J. Li, and S. Yan, Effects of different concentrations of ascorbic acid on the stability of (+) – Catechin under enzymatic conditions, Food Chem. **399**, 133933 (2023), https://doi.org/10.1016/j.foodchem.2022.133933

[4] C. Creutz, Complexities of ascorbate as a reducing agent, Inorg. Chem. **20**(12), 4449–4452 (1981), https://doi.org/10.1021/ic50226a088

[5] M. Lapes, J. Petera, and M. Jirsa, Photodynamic therapy of cutaneous metastases of breast cancer after local application of meso-tetra-(para-sulphophenyl)-porphin (TPPS4), J. Photochem. Photobiol. B **36**(2), 205–207 (1996), https://doi.org/10.1016/S1011-1344(96)07373-3

[6] Z. Jia, H. Deng, and M. Pu, Synthesis and preliminary biological studies of the novel conjugate ^{188}Re-labeled *meso*-tetrakis(4-sulfophenyl) porphyrin in mice, Nucl. Med. Biol. **34**(6), 643–649 (2007), https://doi.org/10.1016/j.nucmedbio.2007.05.006

[7] S. Binder, H. Kolarova, K. Tomankova, R. Bajgar, A. Daskova, and J. Mosinger, Phototoxic effect of $TPPS_4$ and $MgTPPS_4$ on DNA fragmentation of HeLa cells, Toxicol. In Vitro **25**, 1169–1172 (2010), https://doi.org/10.1016/j.tiv.2010.11.005

[8] F.S. Pessoto, N.M. Inada, M. Nepomuceno, A.C. Ruggiero, O.R. Nascimento, A.E. Vercesi, and I.L. Nantes, Biological effects of anionic *meso*-tetrakis (*para-sulfonatophenyl*) porphyrins modulated by the metal center. Studies in rat liver mitochondria, Chem. Biol. Interact. **181**(3), 400–408 (2009), https://doi.org/10.1016/j.cbi.2009.07.012

[9] T.M. Lebepe, R. Maluleke, N. Mgedle, and O.S. Oluwafemi, Porphyrin as a cryoprotectant for graphene oxide-coated gold nanorods to produce conjugated product with improved stability and opto-phototherapeutic properties, Pharmaceutics **15**, 2538 (2023), https://doi.org/10.3390/pharmaceutics15112538

[10] M. Nowak, W. Tryniszewski, A. Sarniak, A. Wlodarczyk, P.J. Nowak, and D. Nowak, Effect of physiological concentrations of vitamin C on the inhibitation of hydroxyl radical induced light emission from Fe^{2+}-EGTA-H_2O_2 and Fe^{3+}-EGTA-H_2O_2 systems in vitro, Molecules **26**(7), 1993 (2021), https://doi.org/10.3390/molecules26071993

[11] G.A. Gamov, D.N. Yarullin, M.A. Gudyrina, E.I. Pogodina, A.S. Medvedeva, and M.N. Zavalishin, Protonation of L-ascorbic acid in an aqueous solution at T = 298.2 K, p = 0.1 MPa, and I = 0.10–5.0 mol L^{-1} (NaCl), J. Chem. Eng. Data

67, 1358–1364 (2022), https://doi.org/10.1021/acs.jced.2c00034

[12] A. Maršalka, A. Kalnaitytė, T. Biekša, and S. Bagdonas, The combined effects of ascorbic acid and bovine serum albumin on phototransformations of hematoporphyrin derivative in aqueous medium: Absorption and EPR spectroscopy study, Lith. J. Phys. **62**(1), 58–71 (2022).

[13] L.C. Bichara, H.E. Lanús, C.G. Nieto, and S.A. Brandán, Density functional theory calculations of the molecular force field of L-ascorbic acid, vitamin C, J. Phys. Chem. A **114**(14), 4997–5004 (2010), https://doi.org/10.1021/jp912251g

[14] P.G. Magar, R. Uprety, K.B. Rai, First-principles DFT study of the molecular structure, spectroscopic analysis, electronic structures and thermodynamic properties of ascorbic acid, Himal. Phys. **11**, 28–40 (2024). https://doi.org/10.3126/hp.v11i1.65329

[15] R.W. Berg, Investigation of L(+)-ascorbic acid with Raman spectroscopy in visible and UV light, Appl. Spectrosc. Rev. **50**(3), 193–239 (2015), https://doi.org/10.1080/05704928.2014.952431

[16] H.A. Dabbagh, F. Azami, H. Farrokhpour, and A.N. Chermahini, Theoretical study on structure, conformation, stability and electronic transition of C4 and C5 anions of ascorbic acid stereoisomers, J. Mol. Struct. **1061**, 69–75 (2014), https://doi.org/10.1016/j.molstruc.2013.12.077

[17] S. Ebrahimi, H.A. Dabbagh, and K. Eskandari, Nature of intramolecular interactions of vitamin C in view of interacting quantum atoms: The role of hydrogen bond cooperativity on geometry, Phys. Chem. Chem. Phys. **18**(27), 18278–18288 (2016), https://doi.org/10.1039/C6CP01678B

[18] A. Gruodis, N. Galikova, K. Šarka, R. Saulė, D. Batiuškaitė, and G. Saulis, Mechanism of intermolecular electron transfer in bionanostructures, in: *Nanodevices and Nanomaterials for Ecological Security*, NATO Science for Peace and Security Series B: Physics and Biophysics, Ch. 17, eds. Y.N. Shunin and A.E. Kiv (Springer Dordrecht, 2012) pp. 183–189, https://doi.org/10.1007/978-94-007-4119-5_17

[19] A. Gruodis, N. Galikova, K. Šarka, R. Saulė, D. Batiuškaitė, and G. Saulis, On the mechanism of synergistic cytotoxicity of vitamins C and K3: Experiments *in vitro* and quantum-chemical analysis, Biophys. J. **102**(3), 576A (2012).

[20] G.W. Trucks, H.B. Schlegel, G.E. Scuseria, M.A. Robb, J.R. Cheeseman, G. Scalmani, V. Barone, G.A. Petersson, H. Nakatsuji, X. Li, et al., *Gaussian 16, Revision C.01, M.J. Frisch* (Gaussian, Inc., Wallingford CT, 2016).

$TPPS_4$ IR *L*-ASKORBO RŪGŠTIES KOMPLEKSAS: PORFIRINO CENTRO PROTONAVIMAS

A. Maršalka [a], A. Gruodis [a], S. Bagdonas [b]

[a] *Vilniaus universiteto Fizikos fakulteto Cheminės fizikos institutas, Vilnius, Lietuva*

[b] *Vilniaus universiteto Fizikos fakulteto Lazerinių tyrimų centras, Vilnius, Lietuva*

Santrauka

L-askorbo rūgšties ir $TPPS_4$ kompleksas vandenyje yra traktuojamas kaip glaudaus kontakto asociatas (tarpmolekulinis atstumas <0,2 nm). Straipsnyje pateikiamas dviejų tipų kompleksų struktūros ir elektroninio sužadinimo modeliavimas kvantinės chemijos metodais. Abiejuose kompleksuose *L*-askorbo rūgštis veikia kaip reduktorius. Antrajame komplekse [*L*-askorbo rūgštis + $TPPS_4$ + *L*-askorbo rūgštis] vyksta tarpmolekulinė krūvio pernaša. $TPPS_4$ centro protonavimas gali būti realizuotas, prijungus dvi *L*-askorbo rūgšties molekules kaip protonų šaltinius. *L*-askorbo rūgšties buvimas tirpiklyje leidžia efektyviai protonuoti pirminę struktūrą: $TPPS_4 \rightarrow H_2TPPS_4$.